Nuclear Engineering and Design 106 (1988) 345–355
North-Holland, Amsterdam

RESPONSE OF NPP STRUCTURES TO SIMULTANEOUSLY ACTING AIR PRESSURE LOADS AND GROUND WAVES CAUSED BY A GAS CLOUD EXPLOSION

H. WERKLE and G. WAAS

Hochtief A.G., Abt. KTI, Bockenheimer Landstr. 24, 6000 Frankfurt/Main 1, Fed. Rep. Germany

Received 22 June 1987

Gas cloud explosions cause air pressure waves which propagate over the ground surface. The ground motion induced by these loads and their effect on structures are studied. The soil is modelled as a linear viscoelastic medium. A semianalytical method is used to compute the ground motion produced by a deflagration and by a detonation in a stiff and a soft layered soil. For a PWR reactor building subjected to the direct impact of an air pressure wave the additional effects of the ground waves on the motion of the building are studied. Whereas the vertical structural response is increased, the horizontal response decreases, when the effect of the ground waves is included. For the case studied the additional effect of the ground waves is small.

1. Introduction

Nuclear power plants in the Federal Republic of Germany have to be designed for the air pressure wave caused by a gas cloud explosion. In the current design procedure for surface structures, only the direct impact of the air pressure wave on the structure is considered [1,2]. However, in addition to the air pressure wave, ground waves load the structure. They are generated by the sweeping of the air pressure wave over the ground. Surface structures are loaded simultaneously by the air pressure wave and the ground waves, whereas underground structures are only subjected to the ground waves, fig. 1. It is therefore of importance to study the characteristics of these ground waves and their influence on the dynamic response of NPP structures.

In a linear analysis, the response of a structure with a rigid foundation can be obtained by superposition of the response caused by the direct airpressure load and that caused by the ground motion. The free field ground motion in the case of an earthquake excitation generally can be assumed to be equal at all points of the soil surface. This results from the assumption of vertically incident seismic waves. For ground motions caused by gas cloud explosions these assumptions are no longer valid as the ground waves are propagating also horizontally and as they are characterised by high frequencies and short wave lengths [3]. Hence kinematic interaction effects must be taken into account. A simple approach to the kinematic interaction problem is to average the free field motion over the foundation area. In this way Rischbieter et al. [4] obtained the excitation for a gas cloud explosion and computed the corresponding response spectra. To assess the influence of the ground waves on the structural response the accelerations obtained from the response spectra can than be compared with the accelerations caused by the direct air pressure impact. However, in the response spectrum the phase relationship between both is lost.

In more sophisticated analyses the soil and the structure can be represented in a single model. In this way Nelson [5,6] analysed embedded structures using finite

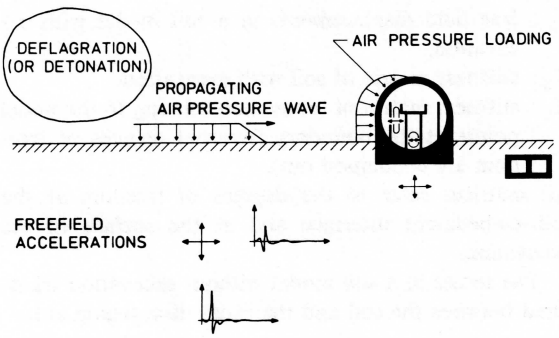

Fig. 1. Loads from a gas cloud explosion.

element and finite difference methods and taking the nonlinear soil behavior into account.

In the present study a semi-analytic method for horizontally layered soils is applied to compute the free field motion as well as the resulting response of a NPP surface structure [7,8]. The analysis of the free field motion is based on a two-dimensional plane strain model. The interaction problem of the structure exited by the free field motion is investigated using an axisymmetric three-dimensional model. Results of the free field motions are given for two soil profiles with stiff and soft soil conditions. To assess the influence of the ground waves a typical PWR building subjected to a gas cloud explosion is analysed with and without simultaneously acting ground excitation.

2. Method of analysis

2.1. Substructuring theorem

For linear systems it is often advantageous to analyse the building and the soil as two separate substructures. In this way, in the simple case of a rigid foundation, the coupling between the soil and the structure reduces to six degrees of freedom and for axisymmetric foundations with plane excitation, as in the present study, to three degrees of freedom. The substructuring principle is formulated in the following for the special case of a soil model which is loaded by propagating surface loads. As the analysis is performed in the frequency domain, the derivation is presented in terms of complex dynamic stiffness matrices.

In the first step the free field displacements are determined for a soil model having an excavation in the region of the embedment of the foundation. The following notations are introduced, fig. 2:

$\boldsymbol{u}_f$: free field displacements in a soil model without excavation,

$\tilde{\boldsymbol{u}}_f$: free field displacements in a soil model with excavation,

$\boldsymbol{K}_S$: stiffness matrix of soil with excavation,

$\boldsymbol{K}_E$: stiffness matrix of excavation relating to the nodal points at the boundary (internal degrees of freedom are condensed out).

All matrices refer to the degrees of freedom at the soil–embedment interface and at the surface of the excavation.

The forces in a soil model without excavation transfered between the soil and the excavation region are:

$$\boldsymbol{K}_E \cdot \boldsymbol{u}_f - \boldsymbol{p}_0, \tag{1}$$

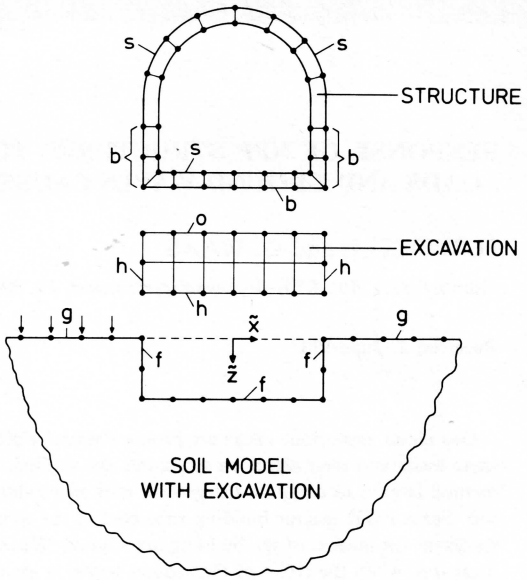

Fig. 2. Substructures.

where $\boldsymbol{p}_0$ are the airpressure forces acting at the surface of the excavated region. If these forces are introduced with opposite sign, the soil–excavation interface becomes free of stresses. The displacements $\hat{\boldsymbol{u}}_f$ resulting from this loading in addition to the free field displacements $\boldsymbol{u}_f$ are the free field displacements $\tilde{\boldsymbol{u}}_f$ in a soil model with excavation. One obtains:

$$\boldsymbol{K}_S \cdot \hat{\boldsymbol{u}}_f = \boldsymbol{K}_E \cdot \boldsymbol{u}_f - \boldsymbol{p}_0, \tag{2}$$

$$\tilde{\boldsymbol{u}}_f = \boldsymbol{u}_f + \hat{\boldsymbol{u}}_f. \tag{3}$$

The second step deals with the displacements of a rigid embedded foundation excited by the free field motion. The rigid body motion of the foundation is described by

$$\boldsymbol{u}_R = \boldsymbol{T} \cdot \tilde{\boldsymbol{u}}. \tag{4}$$

The vectors $\boldsymbol{u}_R$ are the displacements relating to the degrees of freedom at the soil–foundation interface and the surface of the foundation (corresponding to the surface of the excavation). The vector $\tilde{\boldsymbol{u}}$ describes the rigid body motion with in general six and in the present case three degrees of freedom, and $\boldsymbol{T}$ is the rigid body motion transformation matrix. The sum of all forces arising from the relative displacements between the absolute displacements $\boldsymbol{u}_R$ of the foundation and the free field motion $\tilde{\boldsymbol{u}}_f$ must be equal to the forces $\boldsymbol{P}_S$ (with three degrees of freedom here) transfered from the foundation to the structure. This leads to:

$$\boldsymbol{T}^T \cdot \boldsymbol{K}_S \cdot (\boldsymbol{u}_R - \tilde{\boldsymbol{u}}_f) = \boldsymbol{P}_S \tag{5}$$

or with eqs. (2–4):

$$\boldsymbol{T}^{\mathrm{T}} \cdot \boldsymbol{K}_{\mathrm{S}} \cdot \boldsymbol{T} \cdot \tilde{\boldsymbol{u}} = \boldsymbol{T}^{\mathrm{T}}(\boldsymbol{K}_{\mathrm{S}} + \boldsymbol{K}_{\mathrm{E}})\boldsymbol{u}_{\mathrm{f}} - \boldsymbol{T}^{\mathrm{T}} \cdot \boldsymbol{p}_0 + \boldsymbol{P}_{\mathrm{S}}. \tag{6}$$

The matrix

$$\boldsymbol{K}_{\mathrm{R}} = \boldsymbol{T}^{\mathrm{T}} \boldsymbol{K}_{\mathrm{S}} \boldsymbol{T} \tag{6a}$$

contains the complex soil springs, the term $\boldsymbol{T}^{\mathrm{T}} \cdot \boldsymbol{p}_0$ is the sum of the forces acting at the surface of the foundation and the term $\boldsymbol{T}^{\mathrm{T}}(\boldsymbol{K}_{\mathrm{S}} + \boldsymbol{K}_{\mathrm{E}})\boldsymbol{u}_{\mathrm{f}}$ describes the forces acting at the foundation under a free field excitation if the foundation is kept fixed and $\boldsymbol{p}_0$ equals zero.

The coupling of the foundation with the structure leads to the equations of motion of the structure–foundation system:

$$\begin{bmatrix} \boldsymbol{K}_{\mathrm{bb}} & \boldsymbol{K}_{\mathrm{bf}} \\ \boldsymbol{K}_{\mathrm{fb}} & (\boldsymbol{K}_{\mathrm{ff}} + \boldsymbol{K}_{\mathrm{R}}) \end{bmatrix} \cdot \begin{Bmatrix} \boldsymbol{u}_{\mathrm{b}} \\ \tilde{\boldsymbol{u}} \end{Bmatrix} = \begin{Bmatrix} \boldsymbol{P}_{\mathrm{b}} \\ \boldsymbol{T}^{\mathrm{T}}(\boldsymbol{K}_{\mathrm{S}} + \boldsymbol{K}_{\mathrm{E}}) \cdot \boldsymbol{u}_{\mathrm{f}} - \boldsymbol{T}^{\mathrm{T}} \cdot \boldsymbol{p}_0 \end{Bmatrix}. \tag{7}$$

The indices b and f relate to the building and the foundation, respectively. The vector $\{\boldsymbol{u}_{\mathrm{b}}\ \tilde{\boldsymbol{u}}\}^{\mathrm{T}}$ contains the absolute displacements of the building and the foundation and $\boldsymbol{P}_{\mathrm{b}}$ describes the airpressure forces acting externally on the building.

In the present study the displacements in the soil model are described as a sum of cyclic symmetric displacement fields. For a rigid foundation the displacements are completely described by the Fourier terms with $n = 0$ and $n = 1$. Thus the free field displacements $\boldsymbol{u}_{\mathrm{f}}$ and the loads $\boldsymbol{p}_0$ must be transformed into cyclic symmetric components. The equations of motion are then solved separately for $n = 0$ leading to the vertical displacements and for $n = 1$ leading to the horizontal and rocking motion.

2.2. *Stiffness functions of soil*

The soil is modelled as a layer viscoelastic medium which extends horizontally to infinity and is bounded vertically by a rigid base. To solve the equations of motion a semianalytical method is used. In this method the displacement field is approximated in vertical direction by piecewise linear functions and in horizontal direction by the analytic solutions of the equations of motion. Application to the case of a cyclic symmetric ring load acting within or on the surface of the layered medium yields an explicit solution for the displacements, fig. 3. For more details see [7,8].

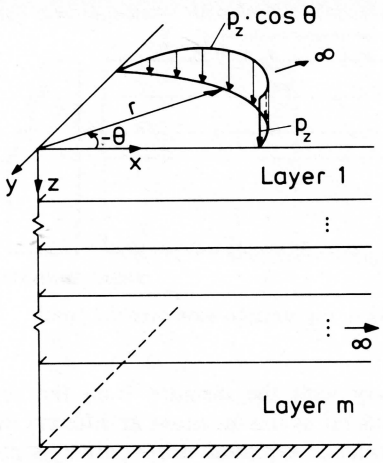

Fig. 3. Ring load solution of a layered medium.

The dynamic flexibility matrix of the nodal rings, at which the soil is to be connected to the structural model, contains the nodal displacements that are produced by unit ring loads applied at each of the nodal rings. Inversion of the flexibility matrix yields the complex dynamic stiffness matrix $(\boldsymbol{K}_{\mathrm{S}} + \boldsymbol{K}_{\mathrm{E}})$ of the layered medium. As the explicit ring load solutions are valid for a horizontally layered medium without an excavation for the structure, the excavation has to be considered separately. To this end the excavated soil is represented by axisymmetric volume elements (torus elements) and the dynamic stiffness matrix $\boldsymbol{K}_{\mathrm{E}}$ is computed for these elements. When this matrix is subtracted from the dynamic stiffness matrix of the layered medium the dynamic stiffness matrix $\boldsymbol{K}_{\mathrm{S}}$ of the soil model with excavation is obtained.

2.3. *Free field motion*

The analysis of the free field motion is based on an explicit solution for the displacements caused by a line load on a layered soil (plane strain). It can be obtained as limit of a ring load solution when the radius of the ring load approaches infinity. Two different derivations are given in [7,10].

The travelling surface loads from air pressure loads are represented by superposition of line loads. For an idealized gas cloud deflagration a pressure time history which increases linearely initially and remains constant after the rise time is assumed. The time history of a detonation is approximated by a function which rises suddenly and then decays exponentially. The pressure peak value as well as the time rate of load increase or

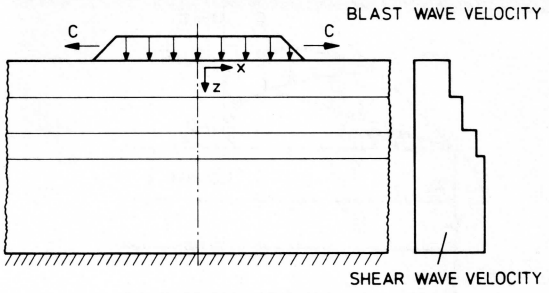

Fig. 4. Air pressure wave over soil profile.

Table 1
Dynamic soil properties, stiff soil profile

Depth [m]	Mass density [kN s^2/m^4]	Shear modulus [MN/m^2]	Poisson ratio ν	Hysteretic damping β
0– 5	1.60	150	0.30	0.05
5– 12	1.90	165	0.48	0.05
12– 30	1.95	220	0.48	0.03
30– 60	2.00	330	0.47	0.03
48– 88	2.05	530	0.46	0.02
88–148	2.10	700	0.45	0.02

decrease vary with the distance from the center of explosion. As far as the functions at different distances from the center of explosion differ only by a phase lag and an amplification factor, the Fourier transform of the load time history has to be performed only once. For loads moving with constant velocity c further numerical simplifications are obtained (see [3,8]). The time history response is obtained using a discrete fast Fourier transformation.

In the following an air pressure wave with plane wave fronts which propagate simultaneously in the positive and negative x-direction is studied, fig. 4.

3. Free field motions in layered soils

3.1. Homogeneous layer

To study the effect of important parameters on the free field ground motion, the simple case of a homogeneous, viscoelastic layer over a rigid base can be considered. For an idealized load function of deflagration type extensive numerical results are presented in [8]. At low air pressure wave velocities ($c < v_R$, v_R = Rayleigh wave velocity in soil) the maximum particle velocities and accelerations in soil increase with the air pressure wave velocity. Maximum response is obtained when the air pressure wave velocity equals the Rayleigh wave velocity in soil. For airpressure wave velocities greater than v_R the maximum particle velocity remains nearly constant and its vertical component is well approximated by an one-dimensional wave propagation analysis (for compressional waves propagating vertically).

3.2. Stiff soil profile

A layered soil with a profile typical for a NPP construction side in a river valley, consisting of sand and gravel is analysed. The shear wave velocity increases from 300 m/s at the surface to 590 m/s at a depth of 80 m, table 1. The total height of the soil model of 160 m is discretized into 24 layers. On the soil surface the discretization interval is 2 m. The Fourier transformation is performed with a period of 3 s and 256 discretization points on the time axis.

First the case of a deflagration is studied in which the air pressure wave propagates with a constant velocity of 340 m/s. The pressure increases in the rise time t_r

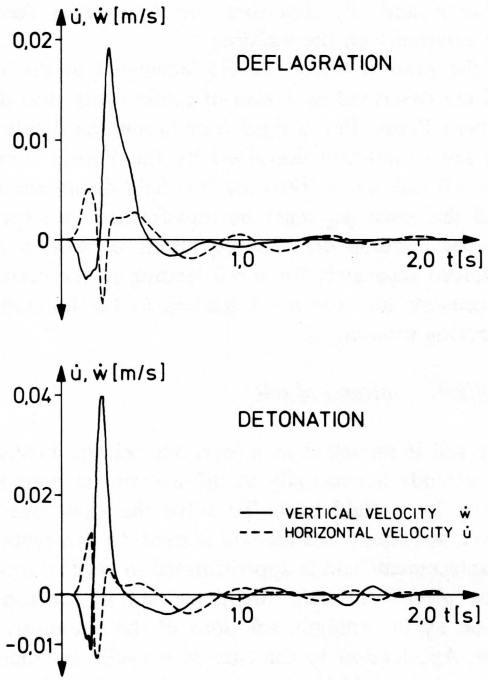

Fig. 5. Particle velocities at ground surface ($x = 64$ m), stiff soil profile.

from 0 to $p = 30$ kN/m^2, where t_r depends on the distance x from the center of explosion:

$$t_r[\mathrm{s}] = 0.0033 \cdot x[\mathrm{m}].$$

These data correspond to a hemispherical gas cloud with a radius of 25 m which is inflamed in their center [4].

The time history of the particle velocity on the soil surface at a distance of 64 m from the center of explosion is shown in fig. 5. It is characterized by a sharp increase of the wave front and a subsequent decaying oscillation, typical for air pressure propagation velocities near to the Rayleigh wave velocity in soil [3]. The vertical and horizontal acceleration response spectra for 5% damping are given in fig. 6 at different distances from the center of explosion. The vertical motions increase with increasing distance from the center of explosion. This reflects the decrease of the loading rate $\dot{p} = p_0/t_r$, where $p_0 = 30$ kN/m^2 remains constant and t_r increases according to eq. (8). The horizontal component is related to the generation of surface waves. Hence, their magnitude relative to the vertical component increases with the distance from the center of explosion.

The peak values of the response accelerations (for $x > 10$ m) are 3 m/s^2 in vertical and 1.6 m/s^2 in

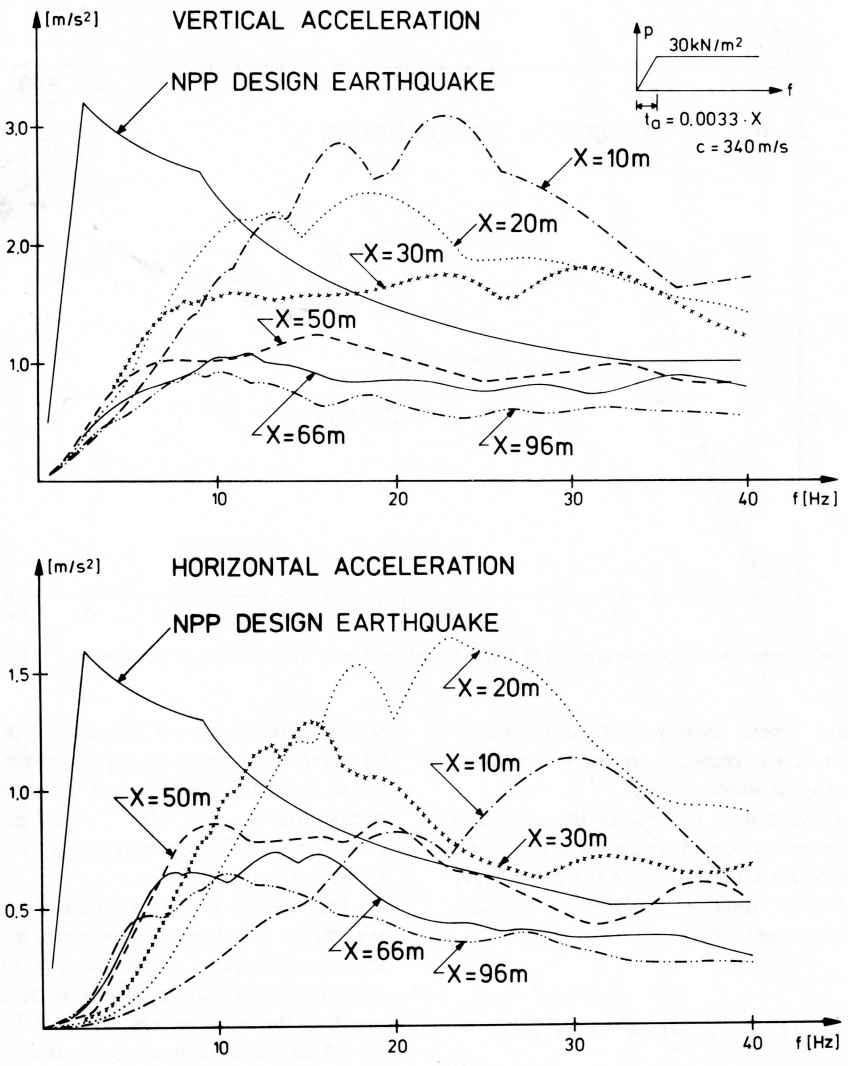

Fig. 6. Free field acceleration response spectra on the surface of the stiff soil profile in the case of a deflagration, 5% damping.

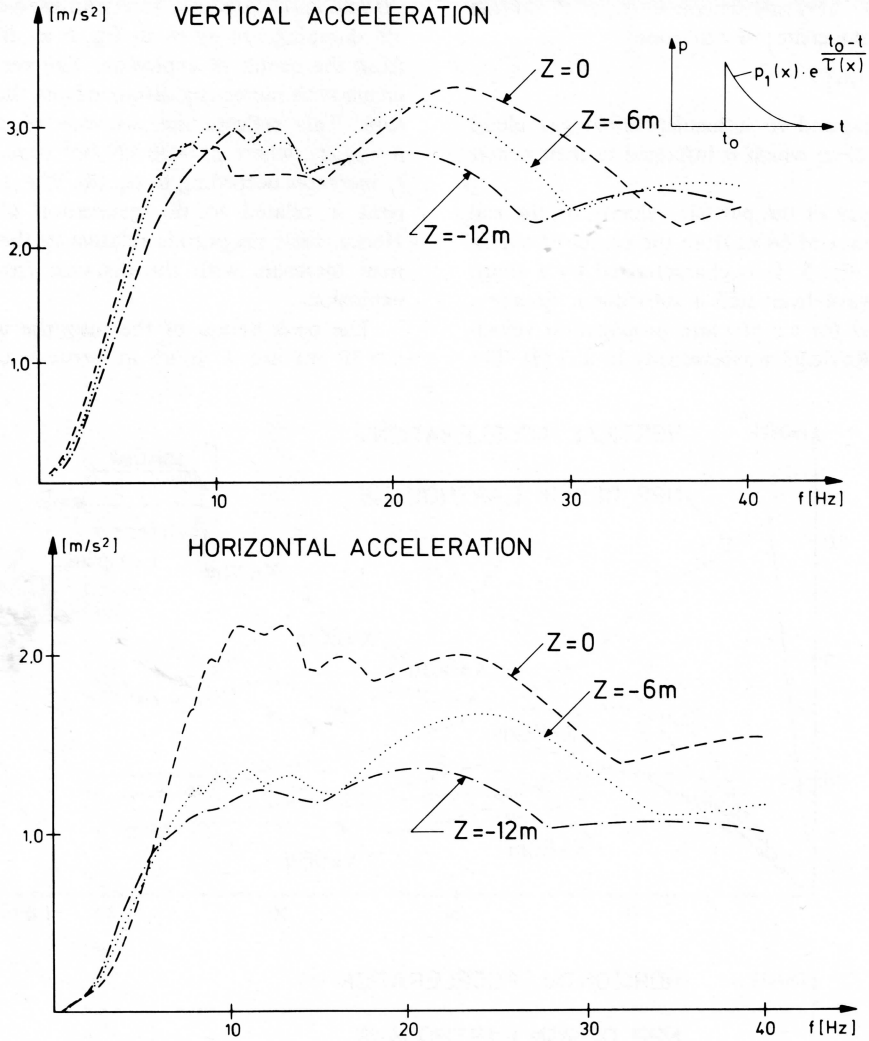

Fig. 7. Free field acceleration response spectra of the stiff soil profile in the case of a detonation, $x = 64$ m, 5% damping.

horizontal direction. These appear in high frequency range of 20–30 Hz. This frequency range is considerably higher than of most earthquakes.

The case of a detonation is studied for the explosion of a ideal hemispherical gas cloud with a radius of 25 m. The air pressure load after the arrival of the airpressure front is described by a function which increases suddenly and decays exponentially:

$$p(x, t) = 0 \qquad t < t_0(x),$$
$$p(x, t) = p_1(x) \exp((t_0 - t))/\tau(x) \qquad t > t_0(x), \tag{9}$$

where t_0 is the arrival time at line x. For a distance of 64 m from the center of explosion the following data are taken according to [4]: peak pressure $p_1 = 34$ kN/m^2, decay time $\tau = 1.5 \times 10^{-2}$ s and propagation velocity $c = 373$ m/s^2. The parameters p_1, τ and c are assumed to be independent on x.

The velocity time histories and acceleration response spectra for 5% damping are given in figs. 5 and 7. They are about twice or three times as high as in the comparable case of a deflagration. In addition to the surface spectra, the spectra for the depths of $z = 6$ m and $z = 12$ m which are usual foundation depths of NPP buildings are computed. The horizontal component of

Table 2
Dynamic soil properties, soft soil profile

Depth [m]	Mass density [kN s^2/m^4]	Shear modulus [MN/m^2]	Poisson ratio ν	Hysteretic damping β
0 –13.9	1.5	6.0	0.49	0.06
13.9–23.4	1.8	82.0	0.49	0.04
23.4–49.4	2.0	155.0	0.48	0.05

motion shows a marked decrease with depth, whereas the vertical component remains constant or increases slightly for low frequencies and decreases for high frequencies. This indicates the importance of surface waves of Rayleigh wave type in the case investigated.

3.3. Soft soil profile

The response of a soft soil, typical for a river valley with alluvial deposits, table 2, is studied. For heavy buildings on the soft soil generally pile foundations are required. The upper 13.9 m of the profile consist of organic soft layers (clay and peat). Underneath are layers of sand and gravel. The soil model has a complete hight of 49.4 m and is discretized in 25 layers. The air pressure loading is the same as for the stiff soil profile.

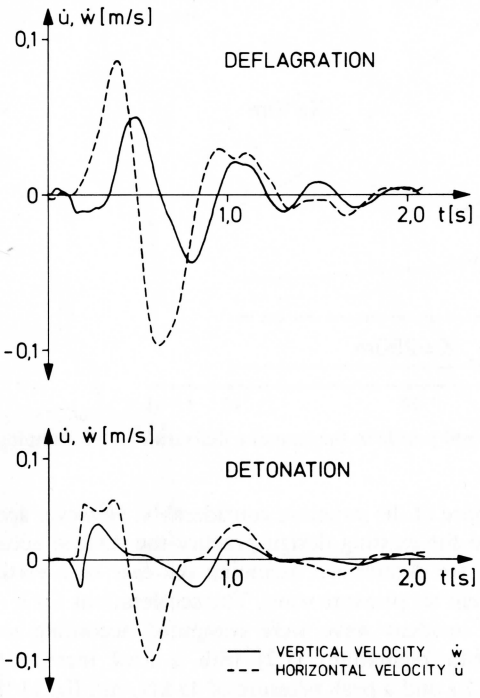

Fig. 8. Particle velocity at the ground surface ($x = 64$ m), soft soil profile.

For a deflagration the time histories of the particle velocities on the soil surface at $x = 64$ m are shown in fig. 8. They are typical for air pressure wave velocities which are high compared to the Rayleigh wave velocity in the soil (see [3]). Because of the smaller impedance $\rho \cdot v_p$ (ρ = density, v_p = compressional wave velocity) the level of the response is considerably higher than in the stiff soil.

The acceleration response spectra at the soil surface in different distances x from the center of explosion are given in fig. 9. They have generally a higher level and more low-frequency components than those for the stiff soil.

4. Response of a PWR building

4.1. Structural model

The response of a building under the wave field excitation is studied for a typical PWR reactor building, fig. 10. It consists of a concrete structure with a spherical steel containment and has a total weight of 1900 MN. Its outer cylinder wall has an external radius of 33 m and is 1.8 m thick. The analysis is performed for the stiff soil profile, table 1.

The structure is modelled as lumped mass model with beam elements, flexible in bending and shear, fig. 11. The flexibility of the base mat is taken into account by an elastic linkage of the external and the internal structure. To compute the structural response in the vertical direction, a simple 2-dof system is used, fig. 12. For both models the first and second eigenfrequencies agree well with those computed with a more sophisticated axisymmetric finite element model of the structure.

The loading function for the case of a deflagration according to section 3.2 is considered. However for the air pressure wave striking the building directly (luff side only), a magnification according to fig. 13 is taken into account, to include wave reflection effects at the building. The resulting forces are obtained by integrating the air pressure over the surface of the building in the hoop direction. The resulting horizontal forces agree well with those according to the German regulations [1], fig. 14a. The vertical force and the overturning moment resulting from the airpressure loading are given in fig. 14b. The

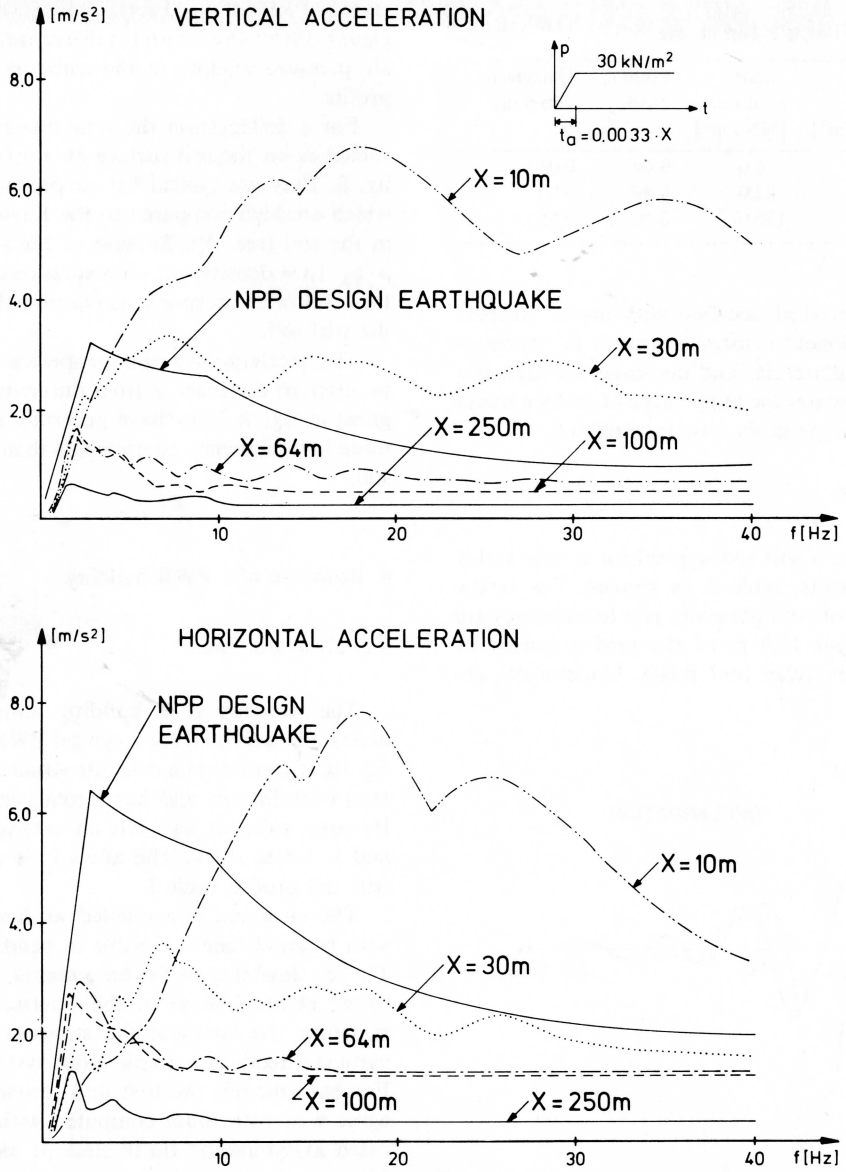

Fig. 9. Free field acceleration response spectra on the surface of the soft soil profile in the case of a deflagration, 5% damping.

center of the explosion is assumed to be 30 m away from the periphery of the building.

4.2. Vertical response

The acceleration time histories of the vertical response of the external structure are given with and without simultaneously acting ground waves in fig. 15. This shows that the ground waves magnify the vertical response of the structure considerably. However according to the existing design practice the vertical accelerations are determined assuming the case of a vertically incident air pressure wave. The accelerations for a vertically incident wave were computed according to the German regulations [1,2] with a load increase time $t = 0.1$ s and a peak pressure of 45 kN/m^2, fig. 11 'luff'. The maxima of the structural accelerations are given in table 3. They are considerably higher than in the case of

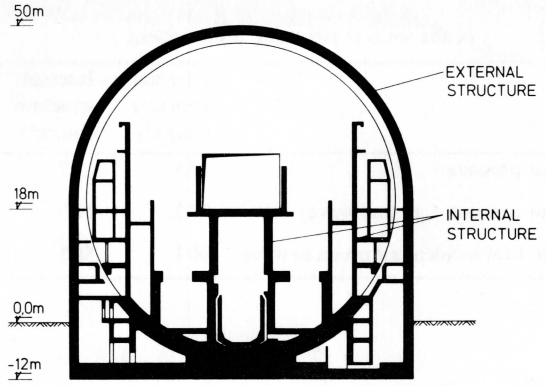

Fig. 10. PWR reactor building.

horizontally propagating air pressure wave, even when the effect of ground waves is included.

4.3. Horizontal response

The loading for the horizontal motion of the building can be decomposed in two parts. The first part are the horizontal air pressure forces, acting on the external

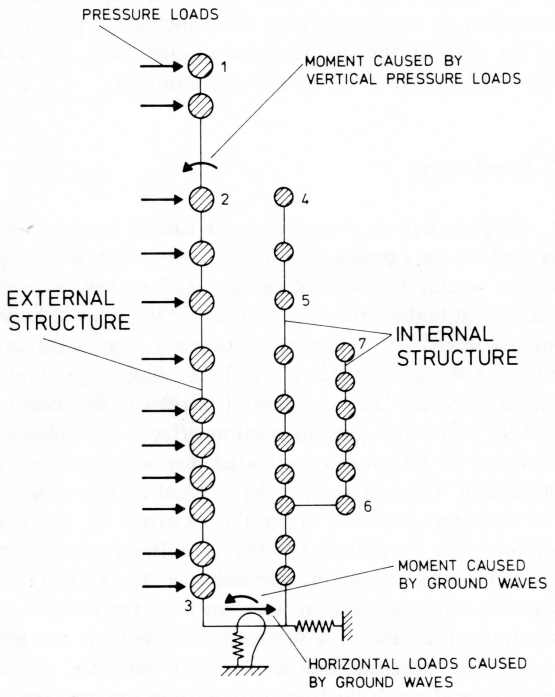

Fig. 11. Structural model for horizontal vibrations.

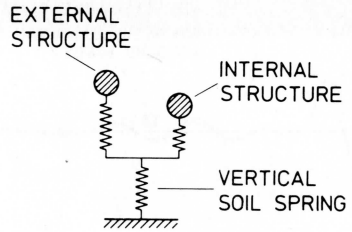

Fig. 12. Structural model for vertical vibrations.

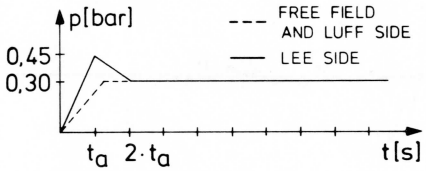

Fig. 13. Air pressure loading on the structure.

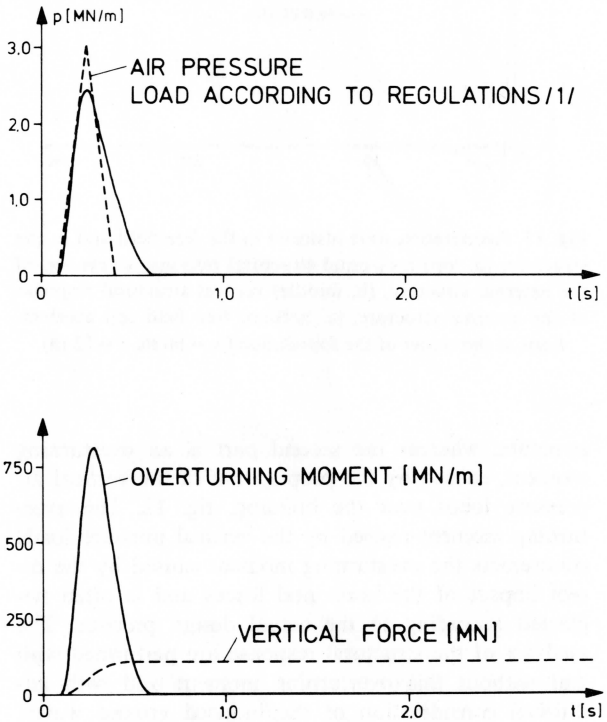

Fig. 14. Resulting air pressure loads on the structure.

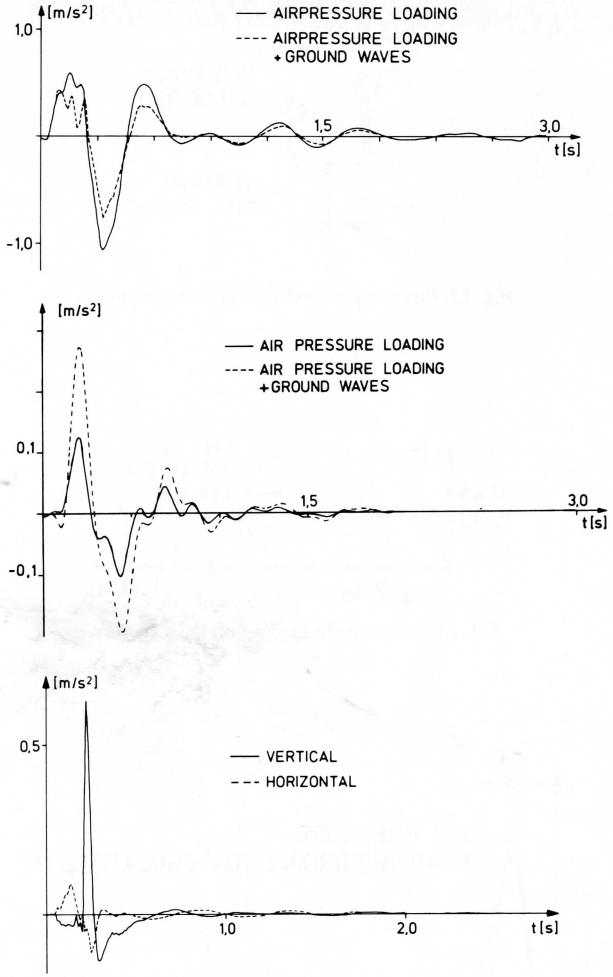

Fig. 15. Acceleration time histories in the free field and in the structure; (a, top) horizontal structural response at the top of the external structure, (b, middle) vertical structural response of the external structure, (c, bottom) free field soil accelerations at the center of the foundation ($x = 66$ m, $z = 12$ m).

structure, whereas the second part is an overturning moment, caused by the propagation of the vertical air pressure loads over the building, fig. 11. The overturning moment caused by the vertical pressure loads counteracts the overturning moment caused by the direct impact of the horizontal forces and is often neglected according to the actual design practice. The analyses of the structural response are performed with and without this overturning moment and with additional consideration of the induced ground waves. Furthermore an analysis according to the German regulations [1,2] with the air pressure function also shown in fig. 13 is performed.

Table 3
Maxima of the vertical structural accelerations

	External structure [cm/s²]	Internal structure [cm/s²]
Air pressure	12.8	7.7
Air pressure + ground wave	27.2	18.5
Vertical incident air pressure wave	90.1	58.1

The acceleration time histories at the top of the external structure of the reactor building are shown in fig. 15. The ground waves amplify the moment caused by the vertical pressure loads and therewith reduce the motion caused by the direct air pressure loading. This yields for all structural points investigated, except the foundation, where the accelerations are slightly increased by the ground waves, table 4.

The maximum structural accelerations according to the German regulations (without consideration of the overturning moment caused by the vertical air pressure loads) are also given in table 4. As the load functions according to the regulations are somewhat higher than in the case of the deflagration studied here, fig. 12a, they lead to greater structural accelerations.

5. Conclusions

Propagating air pressure waves caused by gas cloud explosions may produce ground accelerations with peak values similar to those of design earthquakes but with maxima at higher frequencies. For a PWR reactor building subjected to an air pressure wave, the additional effect of the ground waves on the motion of the building is studied. The horizontal accelerations become smaller when the ground motion effects are included. However in the case investigated, the additional effect of ground waves is small. The vertical accelerations of the building resulting from the external air pressure loading are amplified by the simultaneously acting ground waves. However, according to the existing design practice the vertical accelerations are determined assuming the case of a vertically incident air pressure wave. The accelerations as well as the rate of the vertical load resulting from this assumption are considerably higher than in the case of a horizontally propa-

Table 4
Maxima of the horizontal structural accelerations [cm/s^2]

Loading	Reference points						
	External structure			Internal structure			
	1	2	3	4	5	6	7
Horizontal air pressure loads	124	70	16	52	39	27	42
Horizontal air pressure loads + moment caused by vertical pressure loads	107	60	15	51	37	24	40
Horizontal air pressure loads + moment caused by vertical pressure loads + ground waves	76	51	18	47	32	22	33
Horizontal air pressure loads according to German regulations	192	109	23	84	54	36	59

gating air pressure wave even when the effect of ground waves is included.

Acknowledgements

The authors wish to express their thanks and appreciation for the financial support received from the the Bundesminister für Forschung und Technologie (Contract No. 150 416) and the assistance of the Gesellschaft für Reaktorsicherheit (GRS), Köln, Germany.

References

[1] Richtlinien für die Bemessung von Stahlbetonbauteilen von Kernkraftwerken für Außergewöhnliche Belastungen (Erdbeben, äußere Explosion, Flugzeugabsturz), Institut für Bautechnik, Berlin (1974).

[2] Richtlinie für den Schutz von Kernkraftwerken gegen Druckwellen aus chemischen Reaktionen durch Auslegung der Kernkraftwerke hinsichtlich ihrer Festigkeit und induzierter Schwingungen sowie durch Sicherheitsabstände, Bek. d. BMI v. 1.8.1976, RS I 4-513 145/1.

[3] H. Werkle and G. Waas, Analysis of ground motion caused by propagating air pressure waves, Soil Dynamics and Earthquake Engineering, Computational Mechanics Publications, Southampton, Vol. 6, No. 4 (1987).

[4] F. Rischbieter and K. Michelmann, Bodenwelle bei Gasexplosionen, Beitrag der induzierten Bodenwelle zur Belastung von KKW-Strukturen, Batelle-Institut, Frankfurt (1984).

[5] I. Nelson, Numerical solution of problems involving loading, Proc. Dynamical Methods of Soil and Rock Mechanics, Karlsruhe 1977, Vol. 2 (A.A. Balkema, Rotterdam, 1978).

[6] I. Nelson, Two stage approach to dynamic soil structure interaction, K3/3, SMiRT 6, Paris 1981.

[7] G. Waas, R. Riggs and H. Werkle, Displacement solutions for dynamic loads in a transversely-isotropic stratified medium, Earthquake Engineering & Struct. Dynamics (J. Wiley, Chichester, 1985).

[8] G. Waas and H. Werkle, Response of nuclear power plant structures to the air pressure wave and the induced ground wave caused by gas explosions similar to detonations, Part 2: Induced ground wave, Hochtief AG, Abt. Kerntechnischer Ingenieurbau, Frankfurt (1982), in German.

[9] H. Werkle and G. Waas, Ground waves caused by gas cloud explosions and their effect on nuclear power plant structures, SMiRT7, Chicago, 1983, Paper J10/4.

[10] E. Kausel, An explicit solution for the Green's functions for dynamic loads in layered media, MIT research report R81-13 (1981).